

# First observation of spin dichroism with deuterons up to 20 MeV in a carbon target

V. Baryshevsky, A. Rouba<sup>y</sup>

Research Institute of Nuclear Problems, Bobruiskaya Str.11, 220050 Minsk, Belarus

R. Engels, F. Rathmann, H. Seyfarth, H. Stroher, T. Ullrich

Institut für Kernphysik, Forschungszentrum Jülich, Leo-Bранdt-Str.1, 52425 Jülich, Germany

C. Duweke, R. Emmrich, A. Imig, J. Ley, H. Paetzgen, Schieck, R. Schulze, G. Tendker, C. Wieske  
Institut für Kernphysik, Universität zu Köln, Zulpicher Str.77, D-50937 Köln, Germany

M. M. Mkrtchian, A. Vassiliev  
PNPI, 188300 Gatchina, Russia

The first observation of the phenomenon of deuteron spin dichroism in the energy region of 6-20 MeV is described. Experimental values of this effect for deuterons after passage of an unpolarized carbon target are reported.

PACS numbers: 27.10.+h

## I. INTRODUCTION

It was a long time belief that the phenomena of rotation of the plane of polarization and birefringence applied to photons only. The discovery of neutron spin precession in a polarized target due to the nuclear pseudomagnetic field [1]-[4] and subsequent analyses have shown that analogues of these effects exist not only for photons, but also for other particles [5, 6]. Thus, the optical effects caused by the anisotropy of matter, represent only a special case of the coherent phenomena arising at the passage of polarized particles through matter.

The investigation of spin-dependent interactions of particles is an important part of the research programs to be carried out at storage rings, e.g. RHIC or COSY. The study of a number of phenomena in particle physics demands knowledge of imaginary and real parts of the forward scattering amplitude. Whereas the imaginary part, according to the optical theorem, can be found through the total scattering cross section, the real part may be obtained through dispersion relations or by using the extrapolation of results from small-angle scattering. Thus, the phenomena of birefringence (spin rotation and oscillation) and spin dichroism (defined as the production of spin polarization in an unpolarized beam) of deuterons [5, 6] moving through homogeneous isotropic matter, are of great interest. These phenomena allow the measurement of the real part of the spin-dependent forward scattering amplitude directly. Thus, a check of the dispersion relations on the basis of independent measurements of an im-

aginary and real part becomes possible. Confirmation of the existence of these effects would necessitate taking them into account in all experiments where particles with spins higher than 1/2 are scattered from polarized and unpolarized targets. Especially their contribution in storage rings [7] and for deuteron polarization measurements with thick targets [8] has to be considered. Particularly, considered effect in the residual gas of storage ring should be taken into account for precision EDM measurements [9].

An experiment has been devoted to the first attempt to measure the spin dichroism, i.e. creation of tensor polarization in an unpolarized deuteron beam by unpolarized carbon targets. The experiment has been carried out in the Institute of Nuclear Physics of the University of Cologne using the electrostatic HVEC tandem Van-de-Graaff accelerator with deuterons of up to 20 MeV. A <sup>3</sup>He polarimeter, based upon the reaction  $d + ^3\text{He} \rightarrow ^4\text{He} + p$ , has been used to measure the polarization of the transmitted deuterons.

## II. THEORY: ROTATION AND OSCILLATION OF DEUTERON SPIN IN UNPOLARIZED MATTER (BIREFRINGENCE AND SPIN DICHROISM)

According to [5, 6] the index of refraction of the deuteron (spin S=1) can be written as:

$$\hat{N} = 1 + \frac{2}{k^2} \hat{f}(0); \quad (1)$$

where  $\hat{f}(0) = \text{Tr}_{\text{J}} \hat{F}(0)$ ,  $\hat{f}$  is the density of matter (the number of scatterers in  $1 \text{ cm}^3$ ),  $k$  is the deuteron wave number,  $\hat{F}_{\text{J}}$  is the spin density matrix of the

E-mail: bar@inp.minsk.by; v\_baryshevsky@yahoo.com

<sup>y</sup>E-mail: rouba@inp.minsk.by

scatterers,  $\hat{F}(0)$  is the operator of the forward scattering amplitude, acting in the combined spin space of the deuteron and scatterer's spin  $J$ .

For an unpolarized target  $\hat{F}(0)$  can be written as:

$$\hat{F}(0) = d + d_1 S_z^2 : \quad (2)$$

where  $S_z$  is the  $z$  component of the deuteron spin operator. The axis of quantization  $z$  is directed along the  $\mathbf{n} = \frac{\mathbf{k}}{k}$ , where  $\mathbf{k}$  is the particle wave vector. In the particular case of strong interactions, invariant under parity and time reversal, terms containing odd degrees of  $S$  may be omitted.

As a result the refractive index is:

$$\hat{N} = 1 + \frac{2}{k^2} d + d_1 S_z^2 : \quad (3)$$

Thus, the refractive index of deuterons depends on the deuteron spin orientation relative to the direction of deuteron momentum.

Let us designate the magnetic quantum number as  $m$ , then for a particle in the state which is an eigenvalue of the operator  $S_z$  of spin projection on the axis  $z$ , the refractive index is:

$$\hat{N} = 1 + \frac{2}{k^2} d + d_1 m^2 : \quad (4)$$

According to Eq. (4), states of a particles with quantum numbers  $m$  and  $-m$  possess identical refractive indices. As can be seen,  $\langle N(-1) \rangle \neq \langle N(0) \rangle = N(1) \neq N(0)$ : From here follows that for deuterons even an unpolarized target shows spin dichroism: in the process of passage through matter, due to different absorption, the initial unpolarized beam acquires polarization, more precisely, alignment.

It is easy to explain the appearance of two refractive indices for deuterons as follows: The deuteron in the ground state possesses non-spherical shape. As a result the deuteron has different cross sections in a state with spin direction parallel to its momentum  $\mathbf{k}$  ( $\downarrow$ ) and for spin state  $m = 0$  ( $\uparrow$ ):

$$= f_k(0) = \frac{k}{4} \downarrow = f_\uparrow(0) = \frac{k}{4} \uparrow : \quad (5)$$

According to the dispersion relation  $\langle f(0) \rangle = f(0)$  and as a result  $\langle f_\downarrow(0) \rangle \neq \langle f_\uparrow(0) \rangle$ .

The mutual orientation of vectors  $S$  and  $\mathbf{n}$  for cases  $\downarrow$  (a),  $\uparrow$  (b) is shown in Fig. 1.

We shall discuss the spin behavior of a single deuteron in the target first, then the effects on a deuteron beam using the spin density-operator formalism. If the wave function of a deuteron entering a target is  $\psi_0$ , then the wave function of the deuteron after travelling a distance  $z$  in the target is:

$$\psi(z) = \exp(-ik\hat{N}z) \psi_0 : \quad (6)$$

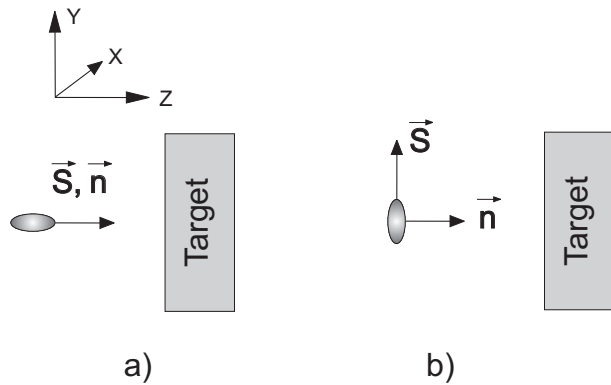


Fig. 1: Mutual orientation of vectors  $S$  and  $\mathbf{n}$  for cases  $\downarrow$  (a),  $\uparrow$  (b).

The wave function  $\psi$  can be represented by a superposition of basis spin functions  $\psi_m$ , where  $\psi_m$  are eigenfunctions of the operators  $\hat{S}^2$  and  $\hat{S}_z$  and  $\hat{S}_z \psi_m = m \psi_m$ :

$$= \sum_{m=1,0,-1} a_m \psi_m : \quad (7)$$

While moving in matter, the spin characteristics of the deuteron (vector and tensor polarization) are changing. The spin state of the deuteron is characterized by a rank-1 (vector) polarization  $\mathbf{p} = h \mathbf{S} \mathbf{i}$  and a rank-2 irreducible tensor moment (in cartesian notation)  $p_{ik} = h Q_{ik} \mathbf{i}$  (tensor polarization).

The knowledge of the explicit form of the spin wave function  $\psi$  of the deuteron is necessary to calculate  $\mathbf{p}$  and  $p_{ik}$ . The wave function of a deuteron as a function of the depth  $z$  in the target is expressed as follows:

$$\begin{aligned} &= \begin{pmatrix} 0 & 1 & 0 & a e^{i k N_1 z} & 1 \\ 0 & a^1 & A = 0 & b e^{i k N_0 z} & A = \\ 0 & a^0 & A = 0 & c e^{i k N_{-1} z} & \\ & a^1 & & & \end{pmatrix} \\ &= \begin{pmatrix} 0 & 1 & & & \\ a e^{i k N_1 z} & & & & \\ 0 & a^1 & 1 & & \\ 0 & a^0 & A = 0 & A = & \\ 0 & c e^{i k N_{-1} z} & & & \end{pmatrix} : \end{aligned} \quad (8)$$

Remember that  $N_1 = N_{-1}$ . Let us choose a coordinate system such that the plane  $(yz)$  coincides with the plane formed by the initial deuteron vector polarization  $\mathbf{p}_0 \neq 0$  and the momentum of the deuteron. In this case  $p_x = 0$ ,  $p_y = 0$ ,  $p_z = \frac{1}{2}$ , and the components of the polarization vector at  $z = 0$  are  $p_x = 0$ ,  $p_y \neq 0$ , and  $p_z \neq 0$ .

Inside the target, the components of the vector  $\mathbf{p} = h \mathbf{S} \mathbf{i} = \frac{h \mathbf{J} \mathbf{j} \mathbf{i}}{h \mathbf{j} \mathbf{i}}$  are:

$$p_x = \frac{p - \frac{2}{2} e^{-\frac{1}{2} (0+1)z} b (a - c) \sin \frac{2}{k} \langle d_1 z \rangle}{h \mathbf{j} \mathbf{i}} ;$$

$$p_y = \frac{p \frac{1}{2} e^{\frac{1}{2} (0+1)z} b (a+c) \cos \frac{2}{k} \langle d_1 z \rangle}{h j i};$$

$$p_z = \frac{e^{-1} z \ a^2 \ c}{h j i}; \quad (9)$$

Similarly, using the cartesian second-rank deuteron spin tensor operator  $\hat{Q}_{ij} = \frac{3}{2} \hat{S}_i \hat{S}_j + \hat{S}_j \hat{S}_i - \frac{4}{3} \delta_{ij}$ ; the components of the tensor polarization are:

$$p_{xx} = \frac{\frac{1}{2} a^2 + c^2 e^{-1} z + b^2 e^{-0} z - 3a\omega e^{-1} z}{h j i};$$

$$p_{yy} = \frac{\frac{1}{2} a^2 + c^2 e^{-1} z + b^2 e^{-0} z + 3a\omega e^{-1} z}{h j i};$$

$$p_{zz} = \frac{a^2 + c^2 e^{-1} z - 2b\omega e^{-0} z}{h j i};$$

$$p_{xy} = 0;$$

$$p_{xz} = \frac{\frac{3}{2} e^{\frac{1}{2} (0+1)z} b (a+c) \sin \frac{2}{k} \langle d_1 z \rangle}{h j i};$$

$$p_{yz} = \frac{\frac{3}{2} e^{\frac{1}{2} (0+1)z} b (a-c) \cos \frac{2}{k} \langle d_1 z \rangle}{h j i}; \quad (10)$$

where  $h j i = a^2 + c^2 e^{-1} z + b^2 e^{-0} z$ ,  $0 = \frac{4}{k} = f_0$ ,  $1 = \frac{4}{k} = f_1$ ,  $f_0 = d$ ,  $f_1 = d + d_1$ .

According to Eqs. (9,10), rotation occurs if the angle between the polarization vector and the momentum of the particle is distinct from  $\frac{\pi}{2}$ .

For example, if  $\langle d_1 \rangle > 0$ , then at an acute angle between the polarization vector and the momentum, the spin will describe a left-handed screw with the direction of momentum, whereas at an obtuse angle between the polarization vector and the momentum, the spin rotation will describe a right-handed screw with the direction of momentum.

For a transversely polarized particle with spin, on entering the target, i.e. at  $z = 0$ , we have  $p_x = 0$ ,  $p_y \neq 0$ , and  $p_z = 0$ . In this case  $a = c$ . According to the above analysis the polarization development with  $z$  will be:

$$p_x = 0;$$

$$p_y = \frac{p \frac{1}{2} e^{\frac{1}{2} (0+1)z} 2ba \cos \frac{2}{k} \langle d_1 z \rangle}{h j i};$$

$$p_z = 0;$$

$$p_{xx} = \frac{4a^2 e^{-1} z + b^2 e^{-0} z}{h j i};$$

$$p_{yy} = \frac{2a^2 e^{-1} z + b^2 e^{-0} z}{h j i};$$

$$p_{zz} = \frac{2a^2 e^{-1} z - 2b\omega e^{-0} z}{h j i};$$

$$p_{xz} = \frac{\frac{3}{2} e^{\frac{1}{2} (0+1)z} 2ab \sin \frac{2}{k} \langle d_1 z \rangle}{h j i};$$

$$p_{yz} = 0; \quad (11)$$

These formulas show that for deuterons passing through a target the vector and tensor polarization oscillate with  $z$ .

### III. ROTATION AND OSCILLATION OF DEUTERON SPIN AND SPIN DICHROISM AT AN ENERGY OF 20 MEV

Let us consider the passage of a deuteron beam through unpolarized matter at 20 MeV, typical for low-energy accelerators. The cartesian spin tensor moment expansion of the density matrix for the deuteron beam before a target is written as follows:

$$\hat{\gamma}_0 = \frac{\hat{I}}{3} + \frac{1}{2} p_x \hat{S}_x + p_y \hat{S}_y + p_z \hat{S}_z$$

$$+ \frac{2}{9} p_{xy} \hat{Q}_{xy} + p_{xz} \hat{Q}_{xz} + p_{yz} \hat{Q}_{yz}$$

$$+ \frac{1}{9} p_{xx} \hat{Q}_{xx} + p_{yy} \hat{Q}_{yy} + p_{zz} \hat{Q}_{zz} : \quad (12)$$

The density matrix of the deuteron beam in the target can be written, using Eq. (8), as:

$$\gamma = \begin{pmatrix} 0 & e^{ikzN_1} & 0 & 1 \\ 0 & 0 & e^{ikN_0 z} & 0 \\ 0 & 0 & 0 & e^{ikN_1 z} \\ 0 & e^{ikN_1 z} & 0 & 0 \\ 0 & 0 & e^{ikN_0 z} & 0 \\ 0 & 0 & 0 & e^{ikN_1 z} \end{pmatrix} A \hat{\gamma}_0 \quad (13)$$

then

$$p = h \hat{S} i = \frac{\text{Tr } \hat{S}}{\text{Tr } (\gamma)}; \quad p_{ik} = h \hat{Q}_{ik} i = \frac{\text{Tr } \hat{Q}_{ik}}{\text{Tr } (\gamma)}$$

where  $i; k = x; y; z$ . Applying this equation to all relevant operator components of the cartesian basis for particles with spin 1  $\hat{I}; \hat{S}_x; \hat{S}_y; \hat{S}_z; \hat{Q}_{xx}; \hat{Q}_{yy}; \hat{Q}_{zz}; \hat{Q}_{xy}; \hat{Q}_{xz}; \hat{Q}_{yz}$  [11] and using the first-order approximation  $e^{ikz(N_1 - N_0)} = 1 + ikz(N_1 - N_0)$ , it is possible to express the spatial development of the initial vector and tensor polarization in the target. With the initial parameters of the beam  $p_{x,0}, p_{y,0}, p_{z,0}, p_{xx,0}, p_{yy,0}, p_{zz,0}, p_{xy,0}, p_{xz,0}, p_{yz,0}$ , we have inside the target:

$$p_x = \frac{1 - \frac{1}{2} z (0 + 1) p_{x,0} + \frac{4}{3} \frac{z}{k} \langle d_1 p_{zy,0} \rangle}{\text{Tr } \hat{I}};$$

$$\begin{aligned}
p_y &= \frac{1 - \frac{1}{2} z (0 + 1) p_{y;0} - \frac{4}{3} \frac{z}{k} < d_1 p_{zx;0}}{\text{Tr} \hat{I}}; \\
p_z &= \frac{(1 - \frac{1}{2} z) p_{z;0}}{\text{Tr} \hat{I}}; \\
p_{xx} &= \frac{(1 - \frac{1}{2} z) p_{xx;0} + \frac{1}{3} z (1 - 0) - \frac{1}{3} z (1 - 0) p_{zz;0}}{\text{Tr} \hat{I}}; \\
p_{yy} &= \frac{(1 - \frac{1}{2} z) p_{yy;0} + \frac{1}{3} z (1 - 0) - \frac{1}{3} z (1 - 0) p_{zz;0}}{\text{Tr} \hat{I}}; \\
p_{zz} &= \frac{1 - \frac{1}{3} z (2 - 0 + 1) p_{zz;0} - \frac{2}{3} z (1 - 0)}{\text{Tr} \hat{I}}; \\
p_{xy} &= \frac{(1 - \frac{1}{2} z) p_{xy;0}}{\text{Tr} \hat{I}}; \\
p_{xz} &= \frac{1 - \frac{1}{2} z (0 + 1) p_{xz;0} + 3 \frac{z}{k} < d_1 p_{y;0}}{\text{Tr} \hat{I}}; \\
p_{yz} &= \frac{1 - \frac{1}{2} z (0 + 1) p_{yz;0} - 3 \frac{z}{k} < d_1 p_{x;0}}{\text{Tr} \hat{I}}; \\
\end{aligned} \tag{14}$$

where  $\text{Tr} \hat{I} = 1 - \frac{z}{3} (2 - 1 + 0) - \frac{z}{3} (1 - 0) p_{zz;0}$ :

If the initial beam was unpolarized, i.e.  $p_{x;0} = p_{y;0} = p_{z;0} = p_{xx;0} = p_{yy;0} = p_{zz;0} = p_{xy;0} = p_{xz;0} = p_{yz;0} = 0$ , then after passage through the unpolarized target of thickness  $z$  the deuteron beam acquires the tensor polarization:

$$\begin{aligned}
p_{zz} &= \frac{2}{3} z (1 - 0); \\
p_{xx} &= p_{yy} = \frac{1}{3} z (1 - 0); \\
\end{aligned} \tag{15}$$

The tensor polarization can be expressed by the dichroism  $A$  of the unpolarized target:

$$p_{zz} = \frac{4}{3} A; \quad p_{xx} = p_{yy} = \frac{2}{3} A; \tag{16}$$

where

$$A = \frac{I_0 - I}{I_0 + I} = \frac{z}{2} (1 - 0); \tag{17}$$

where  $I_0$  and  $I$  are the deuteron occupation numbers with a spin projection  $m = 0$  and  $1$ , respectively.

Let us estimate the spin rotation of a deuteron beam at an energy of 20 MeV and the dichroism of an unpolarized carbon target using formulas from [6]:  $10^3 \text{ cm}^3$ ,  $z = 0.1 \text{ cm}$ ,  $< d_1 > = 6 \text{ } 10^3 \text{ cm}^{-1}$ ,  $10^0 = 10^{25} \text{ cm}^2$ , from here  $\theta = 10^3 \text{ rad}$ ,  $A = 10^2$ .

However, since the estimate was based on the non-spherical shape of deuteron in the ground state only, additional effects may occur from spin-spin and Coulomb interactions at low energies.

#### IV. THE EXPERIMENT ON THE DETECTION OF DEUTERON SPIN DICHROISM WITH A $^3\text{He}$ -POLARIMETER

The experiment on the detection of spin dichroism of deuterons in a carbon target was carried out at the accelerator of the Institute of Nuclear Physics of Cologne University. The existing  $^3\text{He}$  polarimeter of the experimental installation was used. Its purpose is to measure all components of the deuteron vector and tensor polarization via anisotropies of the outgoing protons from the nuclear reaction [12, 13]

$$d + ^3\text{He} \rightarrow ^4\text{He} + p. \tag{18}$$

The characteristic feature of this polarimeter is the use of four detectors at polar angles of  $24.5^\circ$  in addition to a fifth detector measuring the emitted protons at an angle of  $0^\circ$ . This detector is sensitive to the  $p_{zz}$ -component of the tensor polarization only [13]. The principle of the tensor polarization (dichroism) measurement is now explained briefly.

The most general form of the differential cross section of a reaction of particles with spin 1 under conservation of parity may be derived from Eq. (12) as follows [12]:

$$\begin{aligned}
I(\theta) &= I_0(0) + \frac{3}{2} p_y A_y(\theta) \\
&+ \frac{2}{3} p_{xz} A_{xz}(\theta) + \frac{1}{3} p_{xx} A_{xx}(\theta) \\
&+ \frac{1}{3} p_{yy} A_{yy}(\theta) + \frac{1}{3} p_{zz} A_{zz}(\theta); \\
\end{aligned} \tag{19}$$

where  $\theta$  is the polar angle of reaction product motion,  $p$  the polarization of the beam, and  $A$  the analyzing power of the reaction.

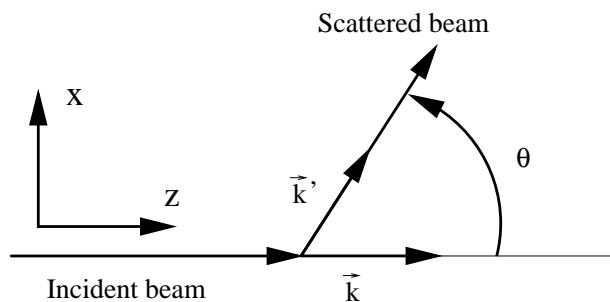


Fig. 2: The system of coordinates.

The system of coordinates for the case considered here is represented in Fig. 2. In this coordinate system the axis of quantization  $z$  is chosen in the direction of the wave vector of the incident beam  $\vec{k}$ , the axis  $y$  along  $\vec{k}^0$  where  $\vec{k}^0$  is the direction of the wave vector of the reaction-product motion, with

the axis  $x$  such that  $x, y$  and  $z$  form a righthanded system.

Of the three components of the beam vector polarization the reaction is sensitive only to the component perpendicular to the scattering plane owing to parity conservation. Similarly, of all nine components of the tensor polarization, owing to parity conservation and the following trace relations, the reaction will be sensitive only to three tensor moment components.

The diagonal elements of the tensor polarization are connected by the trace relation:

$$p_{xx} + p_{yy} + p_{zz} = 0; \quad (20)$$

Similarly for the analyzing power:

$$A_{xx} + A_{yy} + A_{zz} = 0; \quad (21)$$

Thus, only four analyzing-power components are independent. In the above-mentioned system of coordinates the particle scatters to the left if  $\vec{k}$   $\vec{k}^0$  determines the up direction. If we define the azimuthal angle  $\varphi$  as the angle between the plane containing  $\vec{k}$   $\vec{k}^0$  and  $\vec{k}$  and some new plane, also containing  $\vec{k}$ , then we can get a more general formula for the dependence of the differential cross section on the azimuthal angle. The connection of the two coordinate systems [12] is shown in Fig. 3:

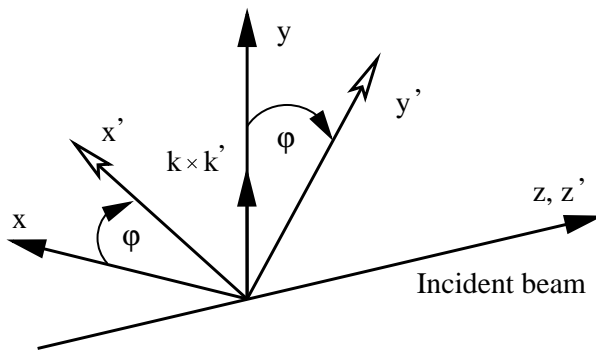


Fig. 3: Orientation of system of coordinates associated with the polarimeter ( $x, y, z$ ) and the system of coordinates associated with the beam ( $x', y', z'$ ). The given case corresponds to the scattering to the left.

$$\begin{aligned} I(\varphi) &= I_0(\varphi) \\ &+ \frac{3}{2} (p_{x^0} \sin \varphi + p_{y^0} \cos \varphi) A_y(\varphi) \\ &+ \frac{2}{3} (p_{x^0 z^0} \cos \varphi - p_{y^0 z^0} \sin \varphi) A_{xz}(\varphi) \\ &+ \frac{1}{6} [(p_{x^0 z^0} - p_{y^0 z^0}) \cos 2\varphi - 2p_{x^0 y^0} \sin 2\varphi] \\ &[A_{xx}(\varphi) - A_{yy}(\varphi)] + \frac{1}{2} p_{z^0 z^0} A_{zz}(\varphi) \quad (22) \end{aligned}$$

Using this general formula, it is possible to write the number of events  $L, R, U, D, F$ , registered by the left ( $\varphi = 24.5^\circ, \varphi' = 0^\circ$ ), right ( $\varphi = 24.5^\circ, \varphi' = 180^\circ$ ), up ( $\varphi = 24.5^\circ, \varphi' = 270^\circ$ ), down ( $\varphi = 24.5^\circ, \varphi' = 90^\circ$ ) and forward ( $\varphi = 0^\circ$ ) detector of the  ${}^3\text{He}$ -polarimeter, respectively:

$$\begin{aligned} L &= N n_L E I(24.5) \\ &+ \frac{3}{2} p_{y^0} A_y(24.5) + \frac{2}{3} p_{x^0} z^0 A_{xz}(24.5) \\ &+ \frac{1}{6} (p_{x^0 z^0} - p_{y^0 z^0}) [A_{xx}(24.5) - A_{yy}(24.5)] \\ &+ \frac{1}{2} p_{z^0 z^0} A_{zz}(24.5) \end{aligned}$$

$$\begin{aligned} R &= N n_R E I(24.5) \\ &+ \frac{3}{2} p_{y^0} A_y(24.5) - \frac{2}{3} p_{x^0} z^0 A_{xz}(24.5) \\ &+ \frac{1}{6} (p_{x^0 z^0} - p_{y^0 z^0}) [A_{xx}(24.5) - A_{yy}(24.5)] \\ &+ \frac{1}{2} p_{z^0 z^0} A_{zz}(24.5) \end{aligned}$$

$$\begin{aligned} U &= N n_U E I(24.5) \\ &+ \frac{3}{2} p_{y^0} A_y(24.5) + \frac{2}{3} p_{x^0} z^0 A_{xz}(24.5) \\ &- \frac{1}{6} (p_{x^0 z^0} - p_{y^0 z^0}) [A_{xx}(24.5) - A_{yy}(24.5)] \\ &+ \frac{1}{2} p_{z^0 z^0} A_{zz}(24.5) \end{aligned}$$

$$\begin{aligned} D &= N n_D E I(24.5) \\ &+ \frac{3}{2} p_{y^0} A_y(24.5) - \frac{2}{3} p_{x^0} z^0 A_{xz}(24.5) \\ &- \frac{1}{6} (p_{x^0 z^0} - p_{y^0 z^0}) [A_{xx}(24.5) - A_{yy}(24.5)] \\ &+ \frac{1}{2} p_{z^0 z^0} A_{zz}(24.5) \end{aligned}$$

$$F = N n_F E I(0) \quad 1 + \frac{1}{2} p_{z^0 z^0} A_{zz}(0)$$

where  $N$  is the areal density of the  ${}^3\text{He}$  target in  $\text{cm}^{-2}$ ,  $n$  the number of incident deuterons, the solid angle, and  $E$  the efficiency of each detector.

The schematic of the polarimeter [13], typical spectra of registered protons produced by deuterons in the  ${}^3\text{He}$  cell, and analyzing powers used to calculate the tensor polarization of the deuteron beam are shown in Figs. 4-8.

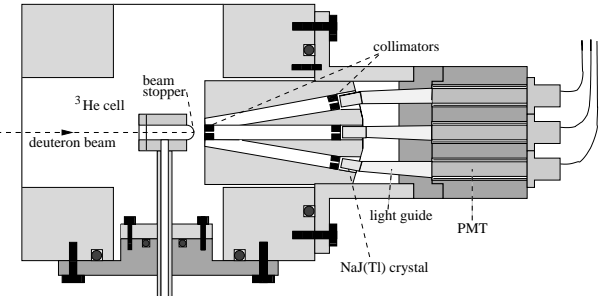
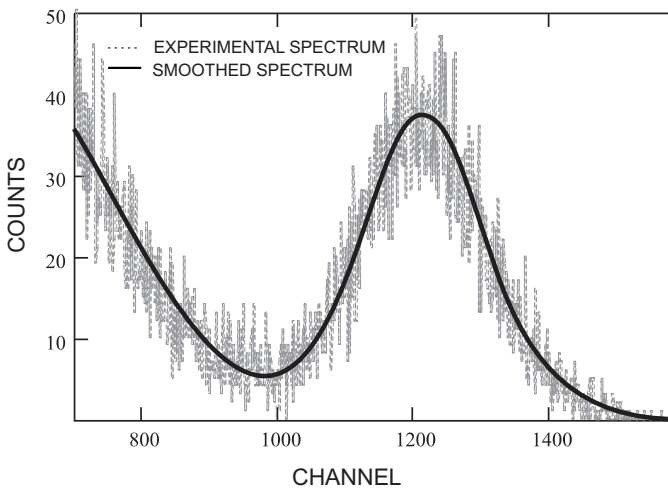
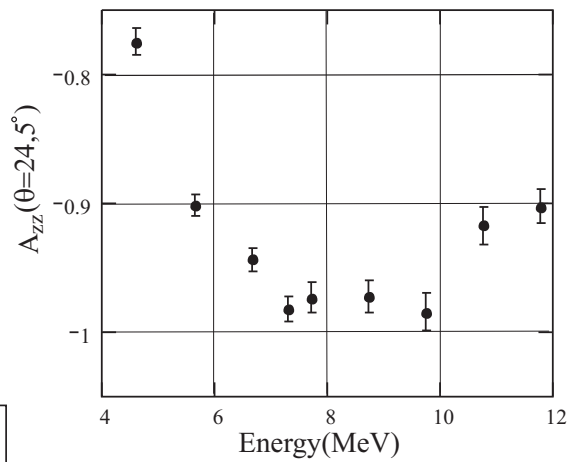
Fig. 4:  $^3\text{He}$ -Polarimeter.Fig. 5: Energy spectrum of protons registered by one side detector, produced by deuterons with an initial energy of 16.2 MeV after passing through the  $151 \text{ mg/cm}^2$  carbon target.

Fig. 7: Analyzing power for the side detectors.

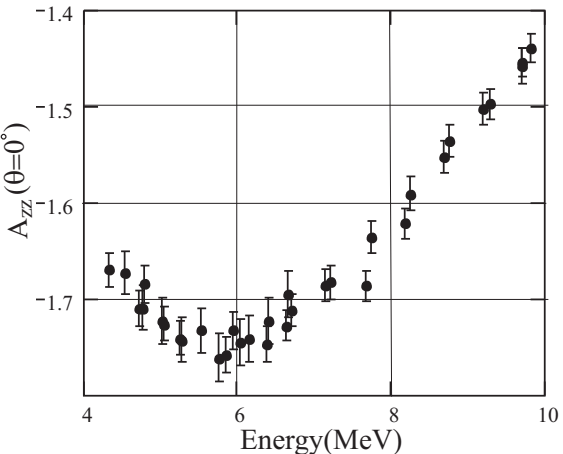
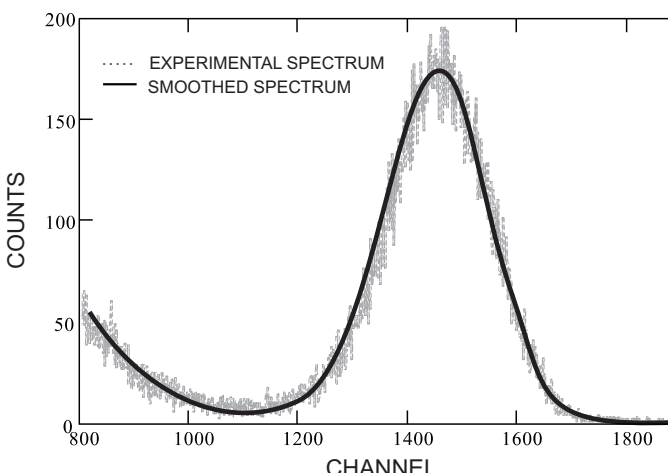


Fig. 8: Analyzing power for the forward detector.

Fig. 6: Energy spectrum of protons registered by the forward detector, produced by deuterons with an initial energy of 16.2 MeV after passing through the  $151 \text{ mg/cm}^2$  carbon target.

## V. DISCUSSION : GENERAL IDEA OF SPIN DICHROISM MEASUREMENT IN VIEW OF $^3\text{He}$ -POLARIMETER FEATURES

In the previous chapters an estimate of the dichroism and tensor polarization of a deuteron beam passing through a carbon target was given. They were about  $10^2$ . This means that the number of particles registered by the detectors after passage of the deuterons through the target should differ from the number of registered particles without a target by  $10^2$ . Of course, this requires that identical numbers of particles were incident on the polarimeter, and their energies identical.

During the experiment some problems were encountered. The first problem is associated with a certain dependence of the detector count rate on beam focusing. Especially with no target the beam crossover has small size and may hit different parts of

the helium cell resulting in a variation of solid angle ratios between different detectors. Thus, individual numbers of registered events in each detector may vary by about 5 %.

Another problem was incomplete secondary-electron suppression in the polarimeter leading to substantial variations of the number of counts for equal charge also depending on focusing.

For these reasons, it was impossible to carry out an accurate energy calibration of the detectors and to obtain an accurate tensor polarization since the differential cross section of the reaction  $d + {}^3\text{He} \rightarrow {}^4\text{He} + p$  strongly depends on energy as shown in Fig. 9 and Fig. 10 [14].

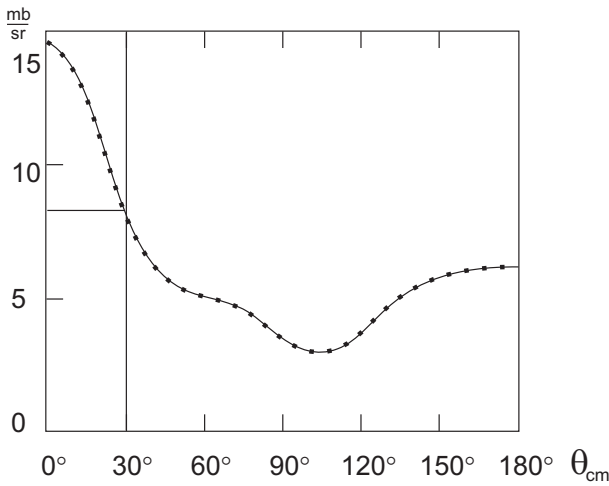


Fig. 9: Differential cross section of the  ${}^3\text{He}(d;p){}^4\text{He}$  reaction at 6 MeV.

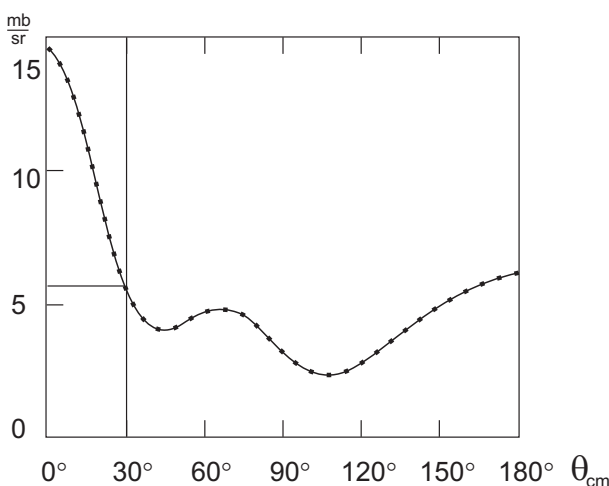


Fig. 10: Differential cross section of the  ${}^3\text{He}(d;p){}^4\text{He}$  reaction at 8 MeV.

Therefore, only an approximate determination of the tensor polarization was possible. In a following experiment the measurement will be improved. It is necessary to choose such combinations of  $L, R, U, D$ ,

$F$  with and without a target such that the results become mainly insensitive to solid-angle variations. Let's designate by  $L_t, R_t, U_t, D_t, F_t$  the number of the registered particles with target, and  $L, R, U, D, F$  without. According to Eqs. (14), (15), after the target the beam has only diagonal components of the tensor polarization  $p_{zz}, p_{xx}, p_{yy}$ , but as  $p_{xx} = p_{yy}$ , we obtain:

$$\begin{aligned}
 L_t &= N n_t L E I(24.5) \cdot 1 + \frac{1}{2} p_{zz} A_{zz}(24.5) \\
 L &= N n L E I(24.5) \cdot 0 \\
 R_t &= N n_t R E I(24.5) \cdot 1 + \frac{1}{2} p_{zz} A_{zz}(24.5) \\
 R &= N n R E I(24.5) \cdot 0 \\
 U_t &= N n_t U E I(24.5) \cdot 1 + \frac{1}{2} p_{zz} A_{zz}(24.5) \\
 U &= N n U E I(24.5) \cdot 0 \\
 D_t &= N n_t D E I(24.5) \cdot 1 + \frac{1}{2} p_{zz} A_{zz}(24.5) \\
 D &= N n D E I(24.5) \cdot 0 \\
 F_t &= N n_t F E I(0) \cdot 1 + \frac{1}{2} p_{zz} A_{zz}^0(0) \\
 F &= N n F E I(0) \cdot 0
 \end{aligned}$$

The relevant combinations used in the data reduction (their variation in this case was about 0.2% ( were therefore:

$$\frac{L + R + U + D}{F} = \frac{(L_t + R_t + U_t + D_t) I(24.5)}{F I(0)} \quad (23)$$

$$\begin{aligned}
 &\frac{L_t + R_t + U_t + D_t}{F_t} \\
 &= \frac{(L_t + R_t + U_t + D_t) I(24.5)}{F_t I(0)} \\
 &\quad \frac{1 + \frac{1}{2} p_{zz} A_{zz}(24.5)}{1 + \frac{1}{2} p_{zz} A_{zz}^0(0)} \quad (24)
 \end{aligned}$$

With  $p_{zz} = 1, A_{zz} = 1$

$$\begin{aligned}
 &\frac{L_t + R_t + U_t + D_t}{F_t} = \frac{L + R + U + D}{F} \\
 &\quad \frac{1 + \frac{1}{2} p_{zz} A_{zz}(24.5)}{1 + \frac{1}{2} p_{zz} A_{zz}^0(0)} \quad (25)
 \end{aligned}$$

i.e., if the beam acquires a tensor polarization in the target this should lead to a change in the ratio of the sum of the number of counts of the side detectors to the counts of the forward detector.

The resulting energy dependence of the experimental points was approximated by a linear least-squares fit. The measurements were carried out with three different targets and the corresponding energies of the incident deuteron beam. The deuteron energies after the targets were found from the Bethe-Bloch formula and should be about 7 MeV. For example a deuteron beam of 18.1 MeV in front of

the carbon target with  $188 \text{ mg/cm}^2$  produces an average beam energy after the target of 7 MeV. At this energy of the incident beam calibration measurements without a target are taken before.

For each target a similar processing of the spectrum was done. The thickness of each target and parameters of the linear  $t$  for each case are shown in table I.

TABLE I: Thickness of targets and parameters of the linear  $t$ .

Target thickness ( $\text{mg/cm}^2$ )	Parameters of linear $t$ $y = kx + b$			
	$k$	$b$		
0	-0.134	0.005	1.72	0.03
57.8	-0.128	0.005	1.68	0.03
151	-0.103	0.006	1.50	0.04
188	-0.116	0.005	1.59	0.03

Experimental points for each target and related linear approximations are represented in Figs. 11–13.

experimental points  $(L+R+U+D)/F$  without target (calibration) / experimental points  $(L+R+U+D)/F$  for targets of  $58 \text{ mg/cm}^2$ ,  $151 \text{ mg/cm}^2$ ,  $188 \text{ mg/cm}^2$ , respectively / linear  $t$  to experimental points  $(L+R+U+D)/F$  without target / ||| { linear  $t$  to experimental points  $(L+R+U+D)/F$  for targets of  $58 \text{ mg/cm}^2$ ,  $151 \text{ mg/cm}^2$ ,  $188 \text{ mg/cm}^2$ , respectively / line corresponding to tensor polarization of  $p_{zz} = 0.1$  independent of deuteron energy .

From the figures and the last table it is visible that straight lines for all cases considered do not coincide. Especially it is evident for the targets of  $151 \text{ mg/cm}^2$  and  $188 \text{ mg/cm}^2$ , i.e. we have different tensor polarization (dichroism) for various target thicknesses. From the figures one more important conclusion follows: the straight line corresponding to tensor polarization 0.1 crosses the straight line corresponding to the unpolarized beam of deuterons with no target in the region of 16 MeV. Experimental data behave very differently, i.e. we have a rather strong dependence of the tensor polarization on the energy of the deuterons.

Experimental points have a relatively wide spread with and without a target, although with target the influence of different focusing conditions should be smaller.

Since the target thickness has an error of 2%, and there is no possibility to calibrate detectors, the error of the deuteron energy after the target, obtained with the Bethe-Bloch formula and tables is 0.2 MeV. This means that the

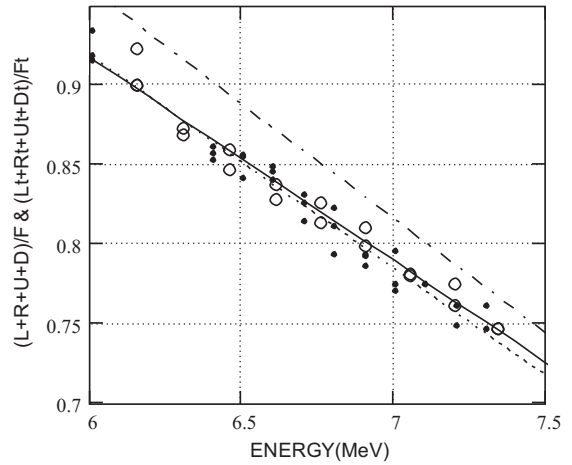


Fig. 11: Energy dependence of  $(L+R+U+D)/F$  without target and  $(L_t+R_t+U_t+D_t)/F_t$  for the target of  $58 \text{ mg/cm}^2$  together with corresponding linear approximations (— experimental points  $(L+R+U+D)/F$  without target (calibration) / — experimental points  $(L+R+U+D)/F$  for targets of  $58 \text{ mg/cm}^2$ ,  $151 \text{ mg/cm}^2$ ,  $188 \text{ mg/cm}^2$ , respectively / — linear  $t$  to experimental points  $(L+R+U+D)/F$  without target / ||| { linear  $t$  to experimental points  $(L+R+U+D)/F$  for targets of  $58 \text{ mg/cm}^2$ ,  $151 \text{ mg/cm}^2$ ,  $188 \text{ mg/cm}^2$ , respectively / — the line corresponding to tensor polarization of  $p_{zz} = 0.1$  independent of deuteron energy ).

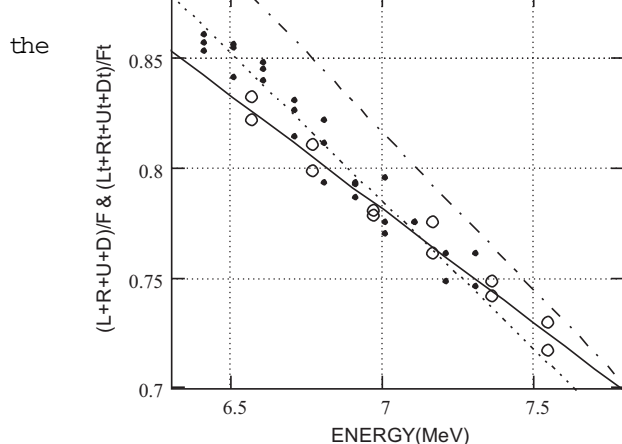


Fig. 12: Energy dependence of  $(L+R+U+D)/F$  without target and  $(L_t+R_t+U_t+D_t)/F_t$  for the target of  $151 \text{ mg/cm}^2$  and corresponding linear approximations (see Fig. 11).

linear relation may be shifted in this interval for each target.

Therefore, a unique source of information about the dichroism (tensor polarization arising) is the

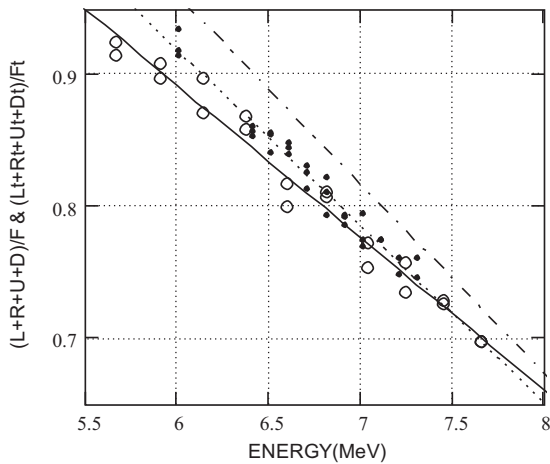


Fig. 13: Energy dependence of  $(L+R+U+D)/F$  without target and  $(L_t+R_t+U_t+D_t)/F_t$  for the target of  $188 \text{ mg/cm}^2$  and corresponding linear approximations (see Fig. 11).

slope of the straight line which does not change essentially in this error interval, i.e. the change of line slope with and without a target testifies to dichroism (tensor polarization) arising according to (25). But since we do not know the deuteron energy after the targets exactly, we cannot find the difference between points on the lines corresponding to the same energy and analyzing power with sufficient accuracy. Though the magnitude of dichroism cannot yet be determined precisely by Eq. (25), from the slope, within its errors, we can conclude that dichroism exists and increases with energy in this energy region. The average dependence of dichroism on deuteron energy after the target passage is shown in Figs. 14-16 where the relation between tensor polarization and dichroism is used:  $A = \frac{3}{4}p_{zz}$ .

## V I. CONCLUSION

From the experimental results it is possible to draw the following conclusions:

1. For all three carbon targeted spin dichroism of deuterons is observed, especially visible for the targets of  $151 \text{ mg/cm}^2$ ,  $188 \text{ mg/cm}^2$ .
2. Dichroism grows in the energy region 6-20 MeV.
3. The sign change of spin dichroism and its not being proportional to the target thickness can

be explained by a more complex dependence of the cross section on the energy of the particles which changes in the process of passage of the beam through the target. For a more complete

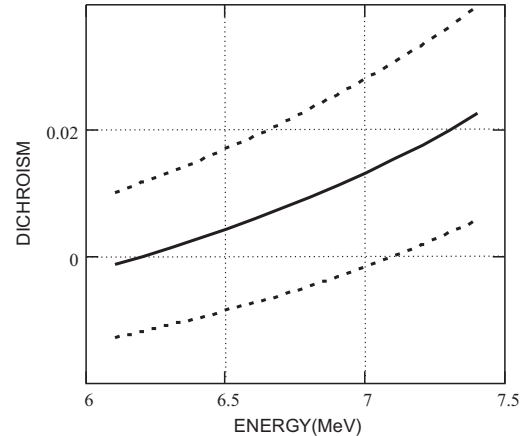


Fig. 14: Dependence of dichroism on deuteron energy after passage of a carbon target of  $58 \text{ mg/cm}^2$  (--- range of deviation).

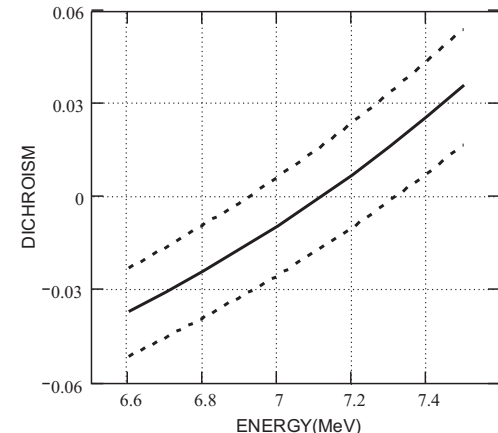


Fig. 15: Dependence of dichroism on deuteron energy after passage of a carbon target of  $151 \text{ mg/cm}^2$  (see Fig. 14).

description of the dichroism observed in this energy region it is necessary to take into account spin-spin and Coulomb interactions, and the possible influence of resonant reactions of deuterons with carbon.

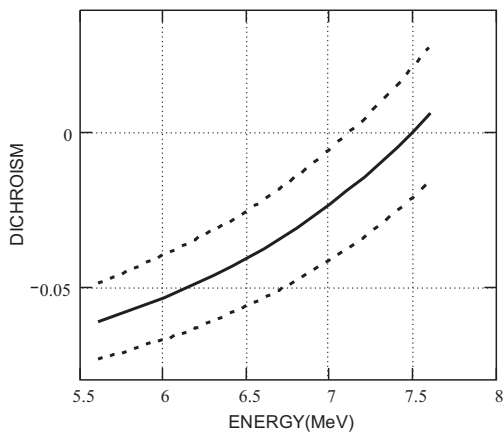


Fig. 16: Dependence of dichroism on deuteron energy after passage of a carbon target of  $188 \text{ mg/cm}^2$  (see Fig. 14).

[3] M. Forte, *Nuovo Cim. A* 18 (1973) 727.

[4] A. Abragam, M. G. Goldsmid, *Nuclear Magnetism: order and disorder* (Oxford Univ. Press, Oxford, 1982).

- [5] V. Baryshevsky, *Phys. Lett. A* 171 (1992) 431.
- [6] V. Baryshevsky, *J. Phys. G* 19 (1993) 273.
- [7] V. Baryshevsky, F. Rathmann, Oscillation and rotation of deuteron spin in polarized and unpolarized targets, COSY summer school, Vol1 (2002).
- [8] S. Kox et al., *Nucl. Instr. and Meth. A* 346 (1994) 527.
- [9] F. J. M. Farley, K. Jungmann, J. P. Müller, W. M. Morse, Y. F. Orlow, B. L. Roberts, Y. K. Senteridis, A. Silenko, and E. J. Stephenson, *Phys. Rev. Lett.* Vol. 93 N. 5 (30 July 2004).
- [10] V. Baryshevsky, K. Batrakov, S. Cherkas, [arXiv:hep-ph/9907464 v1](http://arxiv.org/abs/hep-ph/9907464) (23 July 1999).
- [11] D. Varshalovich, A. M. Osipov, V. K. Hersonsky, *Quantum theory of angular momentum*, Moscow, Science 1975, p.46 (in Russian).
- [12] G. G. Ohlsen, *Polarization transfer and spin correlation experiments in nuclear physics*, *Rep. Prog. Phys.* 35 (1972) 717.
- [13] Diploma thesis, R. Engels, Institut für Kernphysik, Universität zu Köln (1997) <http://www.sikp.uni-koeln.de/3T=arbeiten=engels/diplom.ps.gz> (in German).
- [14] M. Bittcher, W. Gruebler, V. König, P. A. Schmelzbach, B. Vuaridel und J. Ulbricht; *Few-Body Sys.* 9 (1990) 165.